



A spectroscopic census of brown dwarfs observed by Gaia – completing the 3D picture

F. Marocco¹, R. L. Smart², H. R. A. Jones¹, A. C. Day-Jones¹,
B. Burningham¹, and D. J. Pinfield¹

¹ Centre for Astrophysics Research, Science and Technology Research Institute, University of Hertfordshire, Hatfield AL10 9AB, UK, e-mail: f.marocco@herts.ac.uk

² Istituto Nazionale di Astrofisica – Osservatorio Astrofisico di Torino, Via Osservatorio 20, I-10023 Torino, Italy

Abstract. We present the preliminary results of our intended spectroscopic follow-up of the brown dwarfs that will be observed by Gaia. The ESA mission Gaia will observe ~ 500 L0 to L4 dwarfs and a handful of L5 to T1 dwarfs, providing precision of 0.1–0.3 mas in parallax for these objects and tangential velocities at the level of 10–30 m s⁻¹. Here we show the results of our feasibility tests, showing that the wide wavelength coverage and intermediate resolution provided by VLT/X-Shooter is ideal to achieve good precision radial velocities (1–2 km s⁻¹) and to determine spectral indices, identify possible unresolved binaries and members of young moving groups, and further investigate the peculiar objects in the sample. Combined with Gaia results this would be a valuable dataset for many studies.

Key words. brown dwarfs - stars: kinematics and dynamics - astrometry - stars: low-mass

1. Introduction

The ESA cornerstone mission Gaia will revolutionise astronomy observing objects as diverse as minor planets, stars, galaxies out to QSOs and impacting almost all areas of astronomy. We estimate that Gaia will observe directly ~ 500 L0 to L4 dwarfs and a handful of L5 to T1 dwarfs, providing precision of 0.1–0.3 mas in parallax for these objects, distances with relative errors of 1–10% and tangential velocities at the level of 10–30 m s⁻¹ (see Sarro et al., 2013; Smart, 2014). As these objects are very close, the perspective acceleration will change both the parallax and the proper motion over the time frame of the mission, leading to “astrometric” radial velocities

with errors of 10–20 km s⁻¹. However, to fully exploit the extremely accurate and precise astrometric data, it is fundamental to obtain better radial velocities. Therefore we aim to obtain a complete, mid-resolution spectroscopic census of all brown dwarfs that will be observed by Gaia. In this contribution we present the preliminary results obtained in our feasibility test.

2. Science goals

The goal of this project is to complete the medium resolution spectroscopic census of all known brown dwarfs that are within the Gaia magnitude limit. In Figure 1 we plot the distribution in equatorial coordinates (top panel) and

J band magnitude (bottom panel) of the L/T dwarfs that we consider candidates for Gaia observation¹. The majority of the potential targets are within J of 13.5 and 16.5, making them ideal targets for high signal-to-noise ratio spectroscopy. We estimate this distribution is missing 25% of the objects due to incompleteness in the plane.

The spectra will be used to determine radial velocities, spectral indices, identify possible unresolved binaries, and further investigate the peculiar objects in the sample. Combined with the Gaia results this will be an incomparable dataset for many studies. Our knowledge of brown dwarf physical properties often comes from analysis of their spectra. A triangular shape to the H-band peak indicates youth (Lucas et al., 2001), the FeHz and VO indices, and the K I and Na I lines equivalent width can be used to indicate surface gravity (Allers & Liu, 2013), abundances can be estimated via comparisons with benchmark objects and model spectra and line broadening provides rotational velocities.

The holy grail for understanding brown dwarfs has been the associating of individual objects to main sequence stars. When this connection allows us to constrain physical parameters such as age or chemical composition these become benchmark systems (e.g. Zhang et al., 2010; Faherty et al., 2010; Gomes et al., 2013). Gaia will find literally thousands of benchmark systems through the comparison of stellar kinematics and those of brown dwarfs seen, and also not seen by Gaia but observed in ground surveys. In this respect precise radial velocities, and therefore better kinematics, are fundamental to confirm or refute companionship.

Another fundamental contribution comes from members of young moving groups and associations, where the group constraint on the age helps us identifying and characterizing spectral features that are sensitive to surface gravity (e.g. Allers & Liu, 2013). Once again, radial velocities with precisions of 1–2 km s⁻¹ or better are key to identify moving

¹ Source www.dwarfarchives.org. For further details on the selection see Smart (2014)

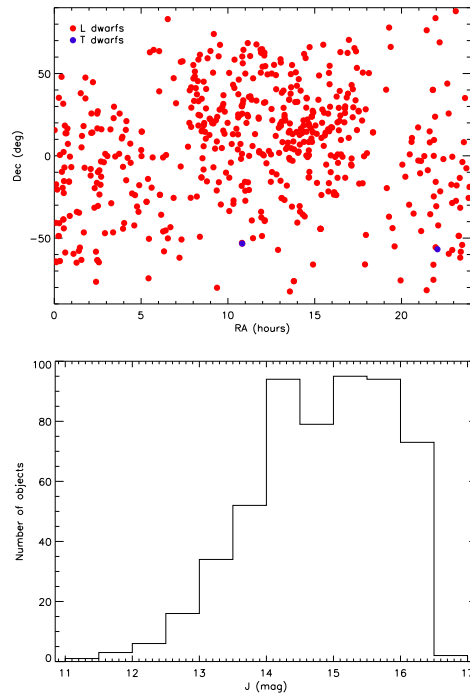


Fig. 1. *Top:* the distribution of brown dwarfs that will be observed by Gaia in the RA–Dec plane. The 547 L dwarfs are plotted in red, and the 2 T dwarfs are plotted in blue. *Bottom:* the distribution in apparent J magnitude. The majority of the potential targets are within J of 13.5 and 16.5, making them ideal targets for high signal-to-noise ratio spectroscopy.

groups members as the groups often overlap in kinematical parameter space (e.g. Gagné et al., 2014; Malo, 2014; Riedel, 2014).

3. Preliminary results

We conducted a preliminary feasibility test using a sample of ~ 190 L and T dwarfs spectra obtained with X-shooter on the Very Large Telescope (Vernet et al., 2011). The sample is presented in Day-Jones et al. (2013) and Marocco et al. (2012) and we refer the reader to these contributions for further details on candidates selection, observation strategy and data reduction procedures.

Using a simple cross-correlation technique we calculated “relative” radial velocities for the objects in the sample. An example of a

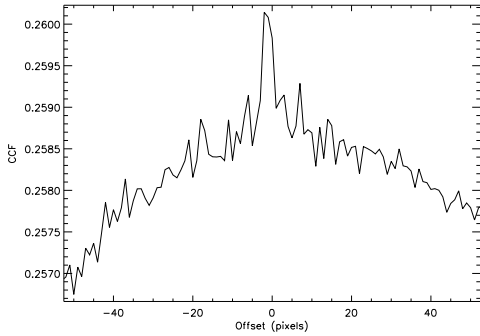


Fig. 2. An example of a cross-correlation function (CCF) obtained for one of our targets. The offset is measured in pixels and then converted into a radial velocity using the wavelength dispersion of the instrument.

cross-correlation function (hereafter CCF) obtained is shown in Figure 2. The CCF shows a clear sharp peak around -1 pix, highlighting the precision of the radial velocity obtained. The exact position of the CCF peak was determined using the procedure described in Taylor (1992) and Press et al. (1986).

The radial velocities have been measured relative to one of the objects in the sample, Kelu-1, that has been selected as “standard” because of its very high signal-to-noise ratio (hereafter SNR) spectrum. The radial velocity of Kelu-1 is given in Blake et al. (2010) and is $6.37 \pm 0.35 \text{ km s}^{-1}$. The results obtained are encouraging, as can be seen in Figure 3, where we plot the precision obtained as a function of the SNR of the spectra, and in Figure 4 where we plot the radial velocity distribution of our targets. In Figure 3 the difference in spectral types between the target and the standard is indicated by the colour of the point, with black points indicating a difference of zero and light grey points indicating a difference of 12 spectral types. Even with an SNR as low as ~ 5 , we can obtain an average precision of $\sim 5 \text{ km s}^{-1}$. Increasing the SNR will allow us to achieve our precision goal of $\sim 1 \text{ km s}^{-1}$. It is clear however that the scatter is very high, and that is probably due to the difference between the late-type targets and the “standard” adopted. In late type objects (i.e. the light grey points in Figure 3)

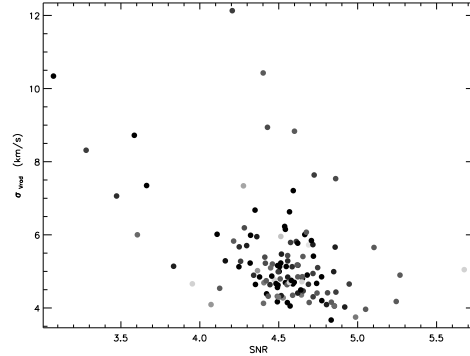


Fig. 3. The distribution of the radial velocity precision obtained as a function of the signal-to-noise ratio (SNR) of the spectra. The difference in spectral types between the target and the standard is indicated by the colour of the point, with black points indicating a difference of zero and light grey points indicating a difference of 12 spectral types. With a SNR as little as ~ 5 we can achieve radial velocity precisions of $4\text{--}6 \text{ km s}^{-1}$.

the Na I and K I lines become shallower and the correlation between the standard and the target is therefore weaker. This would not be a problem in a dedicated radial velocity program, as one would observe standards covering the entire spectral type range, thus reducing the random errors.

Our gaussian fit (plotted as a dotted line in Figure 4) to the distribution peaks at $-1.7 \pm 1.2 \text{ km s}^{-1}$ with $\sigma_{V_{\text{rad}}} = 15.1 \text{ km s}^{-1}$. The distribution we obtained is much narrower than that obtained by Schmidt et al. (2010, overplotted as a dashed line for comparison), who derived $\sigma_{V_{\text{rad}}} = 34.3 \text{ km s}^{-1}$ from a sample of 413 L dwarfs from SDSS. The discrepancy could be due either to the fact that our sample is focused on field (i.e. thin disk) objects, and is therefore biased towards slightly younger dwarfs, i.e. towards a narrower V_{rad} distribution, or to errors in the determination of our radial velocities, introduced by uncorrected instability of X-shooter.

4. Conclusions and future work

The preliminary results of our feasibility test are encouraging. X-shooter seems to be an

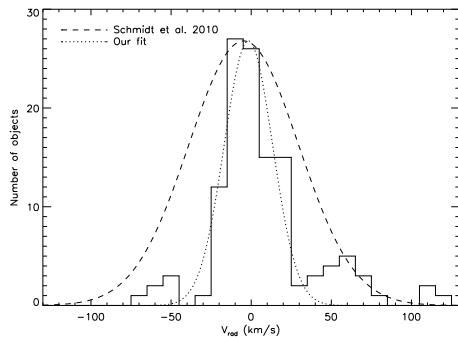


Fig. 4. The radial velocity distribution of our targets. Overplotted as a dashed line is the distribution obtained by Schmidt et al. (2010) from a sample of 413 L dwarfs from SDSS, while the dotted line is our best fit gaussian distribution. Both curves are normalized to the same peak value.

obvious choice to carry on part of the program, given that it combines medium resolution ($R \sim 5000\text{--}9000$) with wide wavelength coverage, observing a large number of absorption lines and bands and therefore increasing the accuracy of the radial velocity measurement. The optical and J band portion of brown dwarf spectra are in fact the richest ones in terms of usable spectral features, and a spectrograph with a resolution of ~ 10000 covering the $0.7\text{--}1.4 \mu\text{m}$ range would be the ideal instrument to conduct our program.

The next steps will be to test the stability of X-shooter (believed to be $\sim 0.5 \text{ km s}^{-1}$ Vernet et al., 2011) using the calibration data available on the ESO archive, and to explore the capability of different present and future instruments (e.g. Caballero, 2014), to complete the campaign on the “northern” targets. The possibility of using different data reduction techniques (e.g. using sky lines instead of arc lamps to improve the wavelength calibration) will also be explored.

Acknowledgements. The authors would like to acknowledge the Marie Curie 7th European

Community Framework Programme PARSEC grant n.236735, and IPERCOOL grant n.247593. FM acknowledges the support of the European Science Foundation GREAT Exchange Grant n.4641. This research is based on observations collected in the ESO programs 086.C-0450(A/B), 087.C-0639(A/B), 088.C-0048(A/B), and 091.C-0452A.

References

- Allers, K. N. & Liu, M. C. 2013, *ApJ*, 772, 79
 Blake, C. H., Charbonneau, D., & White, R. J. 2010, *ApJ*, 723, 684
 Caballero, J.A. 2014, *MmSAI*, 85, 757
 Day-Jones, A. C., Marocco, F., Pinfield, D. J., et al. 2013, *MNRAS*, 430, 1171
 Faherty, J. K., Burgasser, A. J., West, A. A., et al. 2010, *AJ*, 139, 176
 Gagné, J., et al. 2014, *ApJ*, 783, 121
 Gomes, J. I., Pinfield, D. J., Marocco, F., et al. 2013, *MNRAS*, 431, 2745
 Lucas, P. W., et al. 2001, *MNRAS*, 326, 695
 Malo, L., 2014, *MmSAI*, 85, 715
 Marocco, F., et al. 2012, in International conference on stellar libraries, ed. P. Prugniel & H. P. Singh, *Astronomical Society of India Conference Series*, 6, 23
 Press, W. H., Flannery, B. P., & Teukolsky, S. A. 1986, *Numerical recipes. The art of scientific computing* (Cambridge University Press, Cambridge)
 Riedel, A.R. 2014, *MmSAI*, 85, 282
 Sarro, L. M., Berihuete, A., Carrión, C., et al. 2013, *A&A*, 550, A44
 Schmidt, S. J., et al. 2010, *AJ*, 139, 1808
 Smart, R. L. 2014, *MmSAI*, 85, xx
 Taylor, J. H. 1992, *Royal Society of London Philosophical Transactions Series A*, 341, 117
 Vernet, J., Dekker, H., D’Odorico, S., et al. 2011, *A&A*, 536, A105
 Zhang, Z. H., Pinfield, D. J., Day-Jones, A. C., et al. 2010, *MNRAS*, 404, 1817